ANNALI DI GEOFISICA, VOL. XXXVI, N. 1, April 1993

Modeling of the 1980 Irpinia earthquake source: constraints from geodetic data

Folco Pingue(1), Giuseppe De Natale(1) and Pierre Briole(2)
(1) *Osservatorio Vesuviano, Napoli, Italia*
(2) *Istitute de Physique du Globe, Lab. de Seismologie, Paris, France*

Abstract
A model for the 1980 Irpinia earthquake is obtained from levelling data, consistent with all the results obtained by the analyses of the other data sets. The model consists of three fault segments, corresponding to the three main rupture subevents of the main shock. In particular, the inclusion of a small levelling data set located close to the Conza dam put further constraints on the faulting parameters of the third subevent, which was the less constrained by other data sets. A fault almost parallel to the main one, dipping SW (graben model) is the only one compatible with the data. For the second subevent a fault dipping 20° toward NE is strongly supported by levelling data. The total seismic moment released by the three fault segments is 2.6×10^{19} Nm, in good agreement with the seismological estimates by centroid-moment tensor inversion (about 2.7×10^{19} Nm).

1. Introduction

The 1980 Irpinia earthquake is the best documented large earthquake in Italy, and in the whole Mediterranean region. Many research groups have worked on the modeling of this earthquake, using various kinds of data (see for instance Westaway and Jackson, 1984, 1987; Crosson *et al.*, 1986; Bernard and Zollo, 1989; De Natale *et al.*, 1988; Pantosti and Valensise, 1990). Just few months after the event, the main features of this earthquake were already clear, since a lot of data converged toward a well-defined solution for the main fault plane (Arca *et al.*, 1983; Del Pezzo *et al.*, 1983; De Natale *et al.*, 1983). Since the beginning of the research, geodetic data were among the most constraining ones for the gross features of the main fault plane. In particular, they definitively constrained the dip direction of the fault, which was not uniquely determined by seismological data alone (Arca *et al.*, 1983). Although the geodetic lines were not located in such a way to allow a precise location of the fault, when used jointly with the aftershock locations they allowed one to infer the location of the main fault within (2÷5) km. A strong constraint on the fault planes location, and a direct confirmation of the main results obtained from geophysical data, came from the finding of the main fault traces on the ground, by Westaway and Jackson (1984), later completed by Funiciello *et al.* (1988). Crosson *et al.* (1986) and Westaway and Jackson (1987) pointed out the occurrence of multiple events during the main shock. This evidence was further confirmed by Bernard and Zollo (1989), who carefully analyzed various data sets, giving a detailed picture of the space-time evolution of the main shock fracture. Although many features of the fracture mechanism of this event are now very well established, there are still some important questions not well answered, regarding the location and mechanism of the third subevent of the main shock (that occurred 40 s after the nucleation), and the dip and southernmost termination of the main fracture (associated by Bernard and Zollo to the second subevent), that occurred about (18÷20) s after the nucleation. The study of this earthquake has shown in a very clear way that only considering complementary information from many different data sets it is possible to obtain a well-constrained model. In this framework, we reanalyze in this paper geodetic data in the light of the constraints put by other data, and

show that: 1) geodetic data are very consistent with other kinds of data, allowing us to obtain a unique, well-constrained model; 2) they allow us to further refine the model, answering many questions left unresolved by using the other data sets. In particular, using a small set of data not considered in the previous studies, located in the neighborings of the Conza dam (Cotecchia, 1986), it is possible to eliminate the ambiguities on fault location and mechanism of the 40 s subevent (the less constrained one, till now).

2. Geodetic data set and previous results

The main data set consists of 179 vertical deformation data, collected by IGMI (Italian Military Geografic Institute) along the levelling lines shown in fig. 1a)). The last measurements before the earthquake had been performed in 1958-1959; the same lines were then relevelled just after the earthquake. Theoretical measurement errors σ can be approximately described as $\sigma = \sigma_0\sqrt{L}$, where L is the distance (in km) from the reference bench mark and $\sigma_0 = 0.002$ m. Since the first research period after the earthquake, this data set had appeared to be a very powerful tool to infer the gross geometry of the main fault structure, when used together with aftershock locations and focal mechanism obtained by seismological data. In fact, if the aftershock locations gave a good determination of the approximate location of the fault zone (to within 10 km) (fig. 1a)), the focal mechanism from seismological data was not able to define the fault dip, since the two conjugated planes showed almost the same strike, consistent with aftershock epicenter alignment (fig. 1a)). The levelling lines, however, were located in such a way to give a firm statement about the fault dip. In fact, the deformation field showed subsidence up to 0.7 m on almost all the line going from Potenza to Grottaminarda (fig. 1a), 1b)), with the maximum subsidence occurring on the benchmark closest to the alignment defined by the aftershock locations (n. 116 in fig. 1b)). So, although no fault traces had been found yet, the main fault mechanism of this earthquake was soon evident (see Arca *et al.*, 1983; De Natale *et al.*, 1983; De Natale *et al.*, 1985). This mechanism is shown in fig. 1a) and the fit to observed geodetic data in fig. 1b). The overall good agreement of such a simple model with the observed data was remarkable mainly because it represented the first case of Italian earthquake with such a clear mechanism, and for which such a large and varied data set had been collected. Later, the ground fault traces found by Westaway and Jackson (1984) definitively confirmed the main features of this model. However, notwithstanding the overall agreement, figure 1b) evidences some important discrepancies in the predictions of the theoretical model with respect to the observed data (shown by circles in fig. 1b)). For points n. 1 to about n. 15 a long-term local subsidence effect has been recognized, due to the alluvial nature of this soil, affected by packing (Cotecchia, 1986), and in fact these bench marks are too far from the seismogenic structures to be significantly affected by them. In particular, the high gradient of displacement for points n. 121 to n. 125 culminating with successive positive displacement, and the subsidence of points from n. 32 to n. 48, could not be modeled by the single fault model of fig. 1. These difficulties, which indicate a more complex faulting process, were recognized since the first studies (Arca *et al.*, 1983; De Natale *et al.*, 1983; Briole, 1986) and demonstrated that more information was contained in the geodetic data set than the simple gross features of the main faulting episodes. Further research on this earthquake, performed with seismological data sets, pointed out the occurrence of at least 3 different fracture episodes (at 0, 18 and 40 s from the first one), with different mechanisms and locations (see Crosson *et al.*, 1986; Westaway and Jackson, 1987; Bernard and Zollo, 1989; Pantosti and Valensise, 1990). De Natale *et al.* (1988) and Briole (1990) proposed some models, substantially in agreement with all the other data, to fit ground deformations; they also showed that, for the fault segment associated with the 40 s subevent, levelling data (shown by circle 2 in fig. 1b)) could be equally well fitted both by a fault orthogonal to the main fault (as proposed by Crosson *et al.*, 1987), or by a graben model (as proposed by Bernard and Zollo, 1989). In the rest of this paper we use a further levelling data set, consisting of 8 benchmarks located close to the Conza dam (n. 180 to 183 and 188 to 191 in fig. 1). Measurements on this line had been

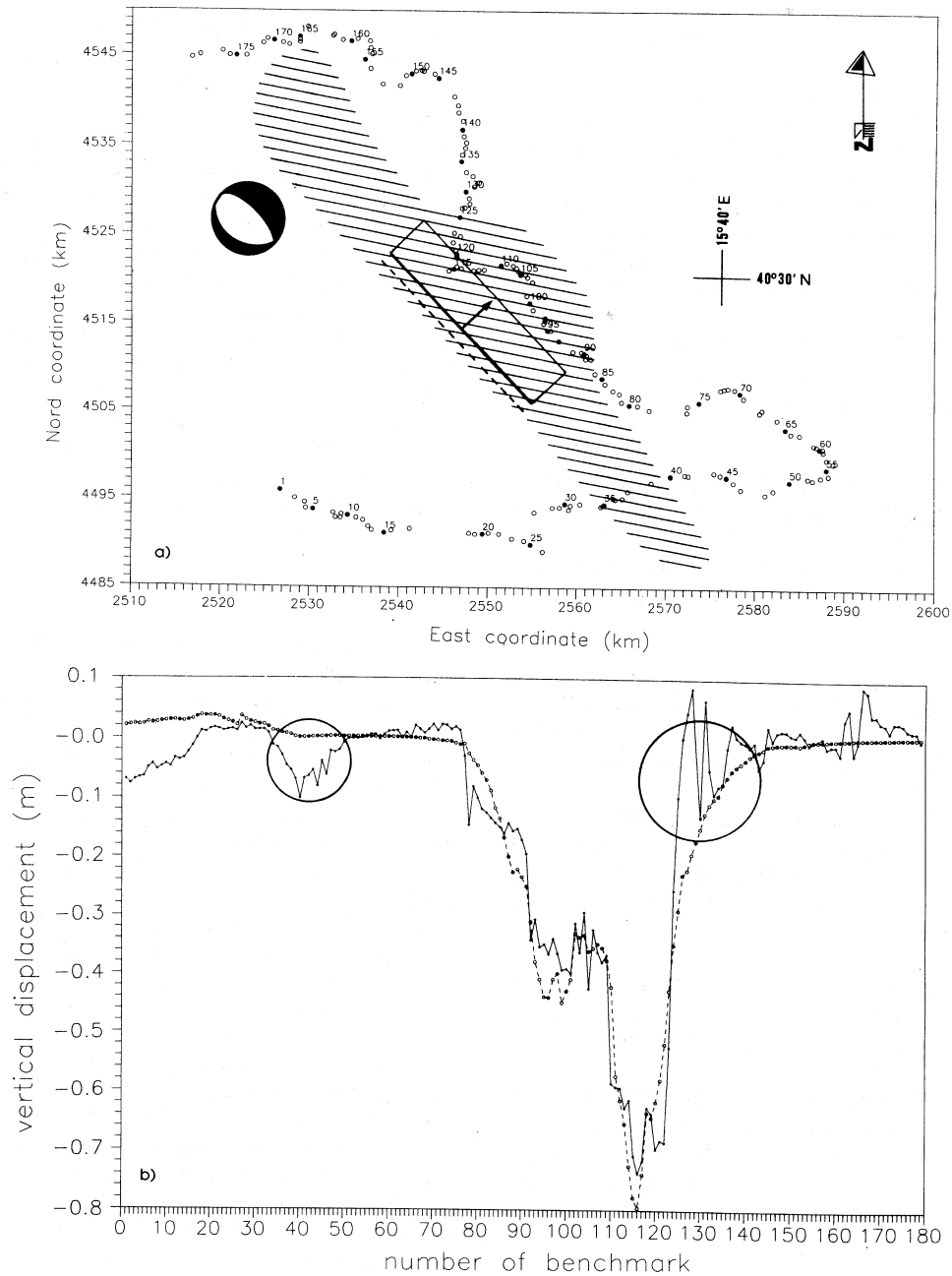

Fig. 1. Best single fault model for the 1980 Irpinia earthquake, from levelling data. a) Fault location (projection at the surface) and levelling lines (circles); the dashed line is the intersection of the fault plane with the surface; the arrow represents the slip direction (dislocation u=2.5 m); the shaded area indicates the aftershock zone. b) Comparison between observed (solid line) and theoretical (dashed line) displacements. Circles on this figure indicate data sets which are significantly misinterpreted by the single fault model.

performed in October, 1980 and were performed again just after the earthquake. These measurements were referred to the IGMI lines, connected through the benchmark n. 121 in fig. 1a). The importance of this data set is evident when looking at their location close to the fault associated to the 40 s event, then representing a very powerful tool to constrain the focal mechanism of this fracture episode. Data from 184 to 187, located on the Conza dam, have not been included in our data set, because the dam was affected by about 0.015 m of nonelastic subsidence due to compaction of shallow layers, consisting of pliocene clays (Cotecchia, 1986).

3. An improved model from geodetic data, with constraints from other data sets

To derive a model for the Irpinia earthquake from levelling data we follow an approach such that:

1) the model must fit the main results obtained from the other types of data; in particular, the fault location must approximately follow the main fault traces, where they intersect the surface.

2) For the features that are not well constrained by other data sets, we will try to explore all the possibilities compatible with levelling data, to see if they can better constrain these features.

The basic model we will refer to is the most widely accepted, consisting of 3 main rupture episodes, occurred at 0, 18 and 40 s from the first shock. We will take as a reference the locations obtained by Bernard and Zollo (1989) for these shocks, in order to compare them with our results. The focal mechanism of the first subevent is assumed known (see fig. 1a)), since it has been confirmed by several data sets and is widely accepted.

3.1. *The 0 s subevent*

The fault location and focal mechanism of this subevent are fixed from the widely accepted results obtained in the literature. The fault termination toward the north is not well constrained by levelling data, and it has been taken as corresponding to the northernmost limit of the fault traces. The only information on this subject obtainable from levelling data is that the termination of the fault must occur before the northernmost lines (n. 150 to 179 in fig. 1b)), which do not show substantial ground displacement. The southernmost termination of the fault is well constrained, because data from 93 to 109 require a strong decrease in slip on the fault to be reasonably fit. The average slip on this fault is almost correlated with that of the 40 s event. It has been computed as giving a total moment of about 1.9 $\times 10^{19}$ Nm, which is higher than that estimated from seismological data (10^{19} Nm). The fault model for this subevent is shown in fig. 2a).

3.2. *The southernmost subevent*

This subevent should correspond to the 18 s subevent as located by Bernard and Zollo (1989). However, since Westaway and Jackson (1987) gave a different location (to the north of the 0 s subevent), we only note that a fault in the zone indicated by Bernard and Zollo (1989) is required by levelling data on the southernmost lines, and it is in agreement with fault traces found in such a zone. The main controversy about this fault is on the dip of the plane, and the southernmost extension. Bernard and Zollo (1989), using the focal mechanism computed by Westaway and Jackson for the 18 s subevent, and the shape of ground deformation, gave a dip of 20° to the fault plane. On the contrary, Pantosti and Valensise (1990) assigned the same dip of the first event to the fault plane. They also state that the southernmost fault termination must be located north the Eboli-Potenza levelling line, because south of it different tectonic domains would be present. Modeling of levelling data helps us to solve these questions. First, we have performed several runs of the direct problem, with sligthly different strikes and position of the fault, in order to infer the best position of the fault, which is strongly constrained in this zone by the subsidence of points 34 through 40. Fault depth has been assumed as 1 km. Once the fault strike has been

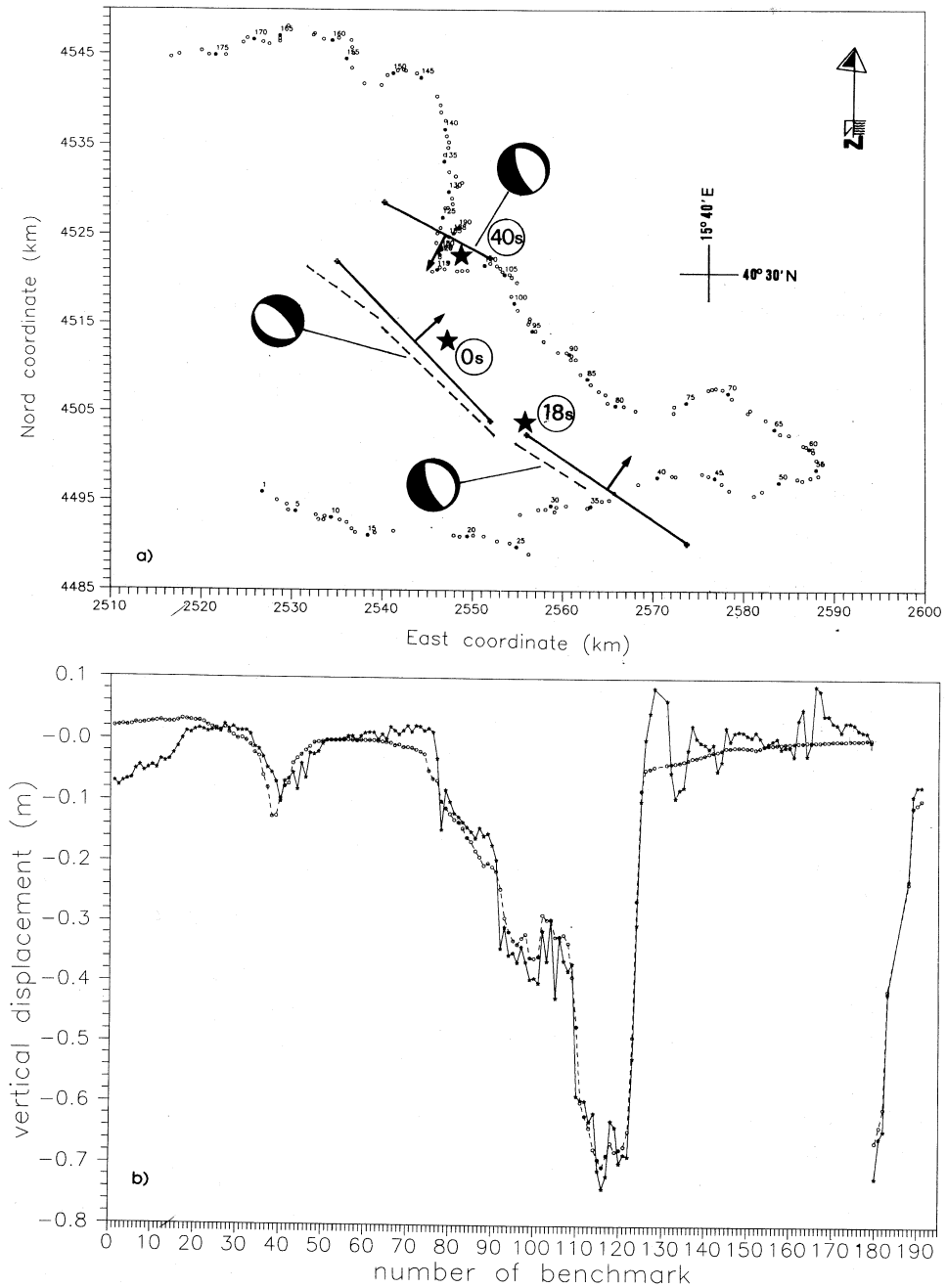

Fig. 2. a) Global fault model obtained in this paper. Circles refer to the subevent locations as computed by Bernard and Zollo (1989). The trend of the fault traces found by Pantosti and Valensise (1990) is indicated by dashed lines. Also shown are the focal mechanisms computed by Westaway and Jackson (1987) for the three main subevents. Fault parameters are given in table I. b) Fit of the model to observed data.

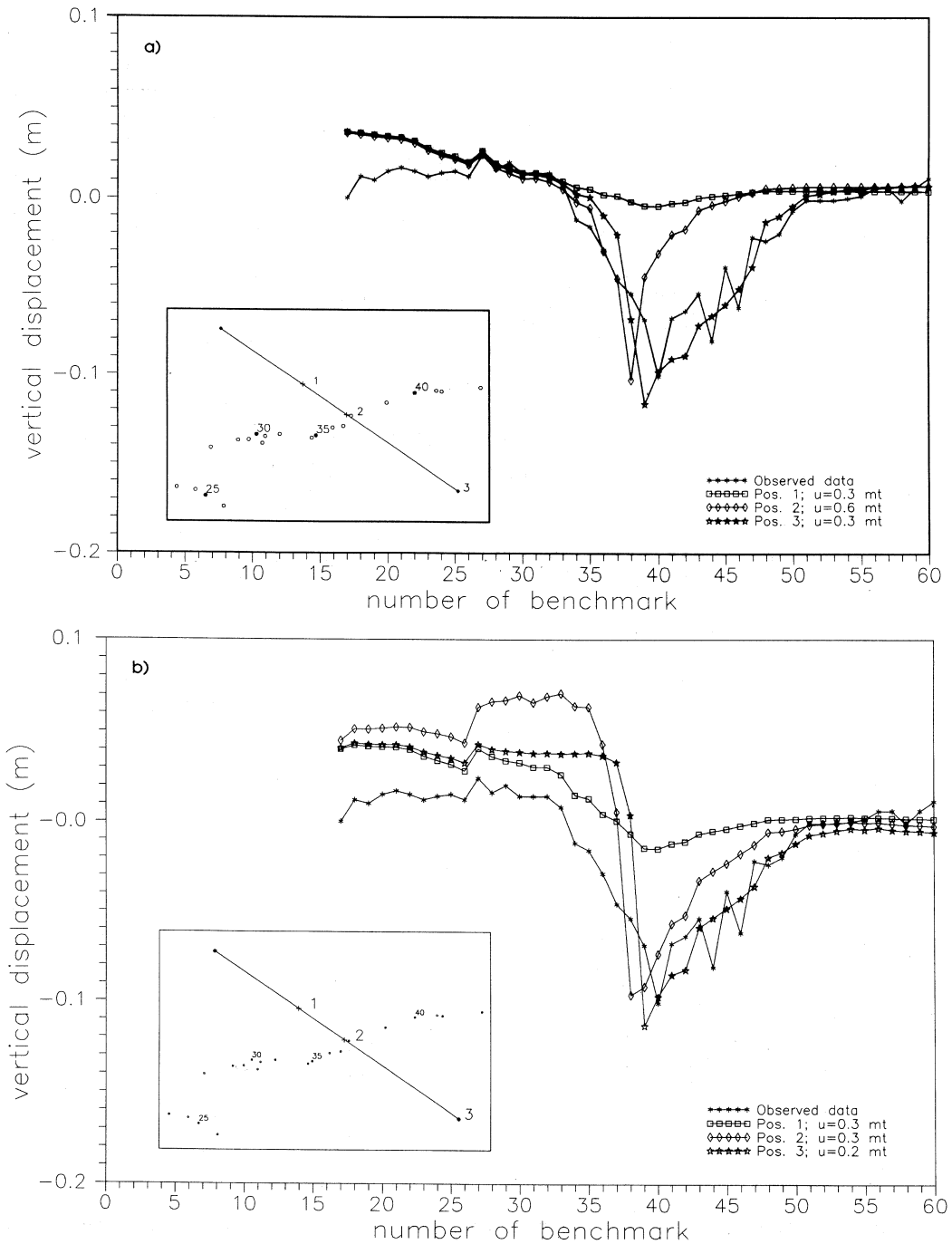

Fig. 3. Fit of observed to theoretical displacements for three different southernmost fault terminations of the 20 s fault (shown in the small box on the left of each figure). a) Dip = 20°. b) Dip = 60°. The depth is 1 km.

inferred, we have examined several possibilities of fault length in order to discriminate the fault dip. In particular, we show in fig. 3 synthetic data computed for a 20° (a)) and a 60° (b)) fault dip for the following cases of the southern termination of the southernmost fault: 1) north of the southernmost levelling line; 2) coinciding with the levelling line; 3) south of the levelling line. As can be seen, a dip of 60° produces ground deformation on the levelling line in strong disagreement with the data, for cases 1) and 2). In these cases, in fact, the displacement on the line has two sharp lobes of different sign, whereas data show exclusively subsidence.

Figure 4 shows the effect of the depth of a fault dipping 60°, for cases from 1) to 3) for the location of the southernmost termination of the fault. Only if the fault termination goes well beyond the levelling line, for depths greater than 3-4 km, the misfit is not too large. However, one should note that in the northern part this fault reaches the surface, so that a depth of 3-4 km or more is difficult to justify. On the contrary, if the dip is 20° or less, the fault model 3) gives a very good fit to the data. Also in this case, however, fault termination must go well beyond the line in order to reproduce the shape of observed data. In the global model of fig. 2 a dip of 20° has been chosen. The seismic moment of the proposed fault model is 3.5×10^{18} Nm, very close to that estimated from seismological data (4×10^{18} Nm).

3.3. *The 40 s subevent*

This event has been probably the most controversial one for many years. First recognized by Crosson *et al.* (1986) from accelerometric records, it was then associated with a normal fault almost orthogonal (N30° E) to the main one. Westaway and Jackson (1987) identified this subevent on teleseismic recordings and computed its focal mechanism, shown in fig. 2a). A scientific debate then issued (see Westaway and Jackson, 1987 and Crosson *et al.*, 1987) about the fracture geometry of this subevent. Bernard and Zollo (1988), on the basis of S-wave polarizations of accelerometric records, computed the best focal mechanism as a fault almost parallel to the main one, dipping NE. Such a mechanism was similar to that proposed by Westaway and Jackson (1987). The dip, however, was not very well constrained, and the same authors (Bernard and Zollo, 1989) later proposed a fault dipping SW (graben model) for this event. De Natale *et al.* (1988) showed that, for modeling geodetic data of the national levelling network owned by the IGMI, a graben model was almost equivalent to an orthogonal fault model. In the last papers on this subject, the graben model has been generally favoured, because better justifiable from a mechanical point of view. We show in the following that the inclusion of a set of levelling data, operated close to the Conza dam, strongly contributes to well constrain the orientation and dip of the fault associated to this subevent. Figure 2a) shows the best model for the 40 s subevent, obtained by inversion of all the available levelling data, by fixing the fault parameters of the other two fault segments to the values inferred in the previous sections. Figure 2b) shows the fit of the model to observed data. It is important to stress that including the new data set rules out models of fault dipping NE and/or with fault orientation orthogonal to the 0 s fault segment. Also the fault width is well constrained, when the the parameters of the 0 s fault are fixed, and the maximum depth (<10 km) is consistent with results obtained by accelerometric studies (Bernard and Zollo, 1989). The seismic moment of this fault is 2.8×10^{18} Nm, in good agreement with seismological data (3×10^{18} Nm).

3.4. *Constraints on strike and dip parameters of the 40 s faulting*

In order to assess the level at which fault strike and dip of this event are constrained by geodetic data, we have computed the sum of square residuals on 48 bench marks (indicated in fig. 5a)) for a complete set of models, by varying strike and slip parameters. The parameters of the other two faults have been fixed to the best model of table I. For the 40 s fault, the length has been fixed to 13 km (as given by our best model); however, the length parameter is not crucial for the results, as shown by several tests performed with different lengths. The depth has been assumed as 1 km, and

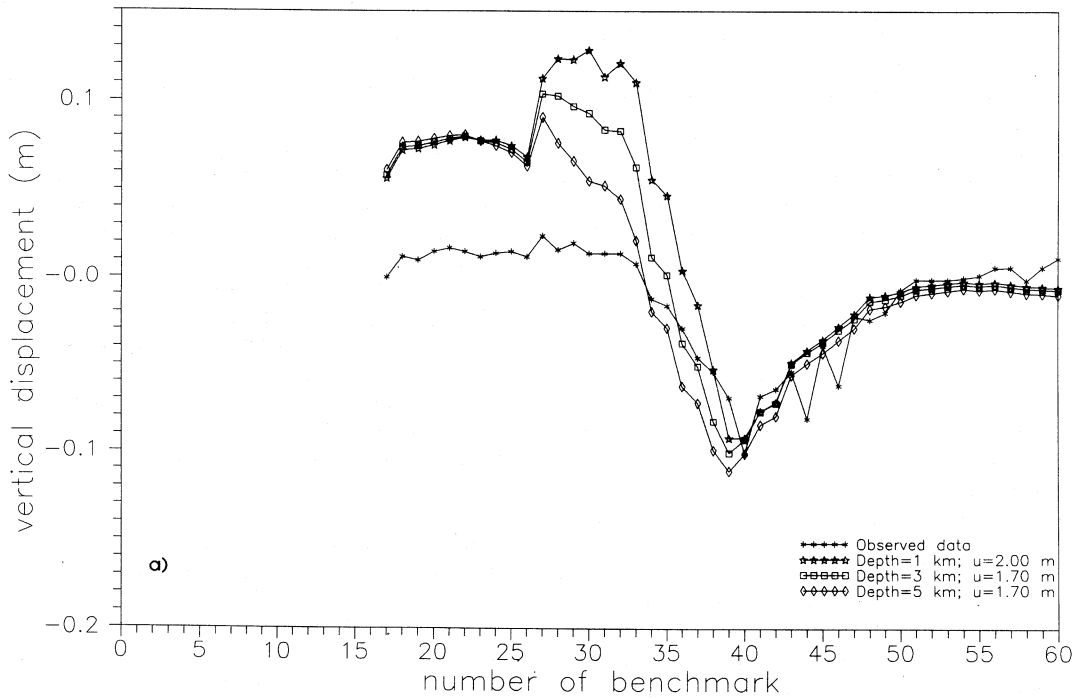
vertical displacement (m)
0.1
−0.0
−0.1
−0.2
0
5
10
15
20
25
30
35
40
45
50
55
60
number of benchmark
a)
Observed data
Depth=1 km; u=2.00 m
Depth=3 km; u=1.70 m
Depth=5 km; u=1.70 m

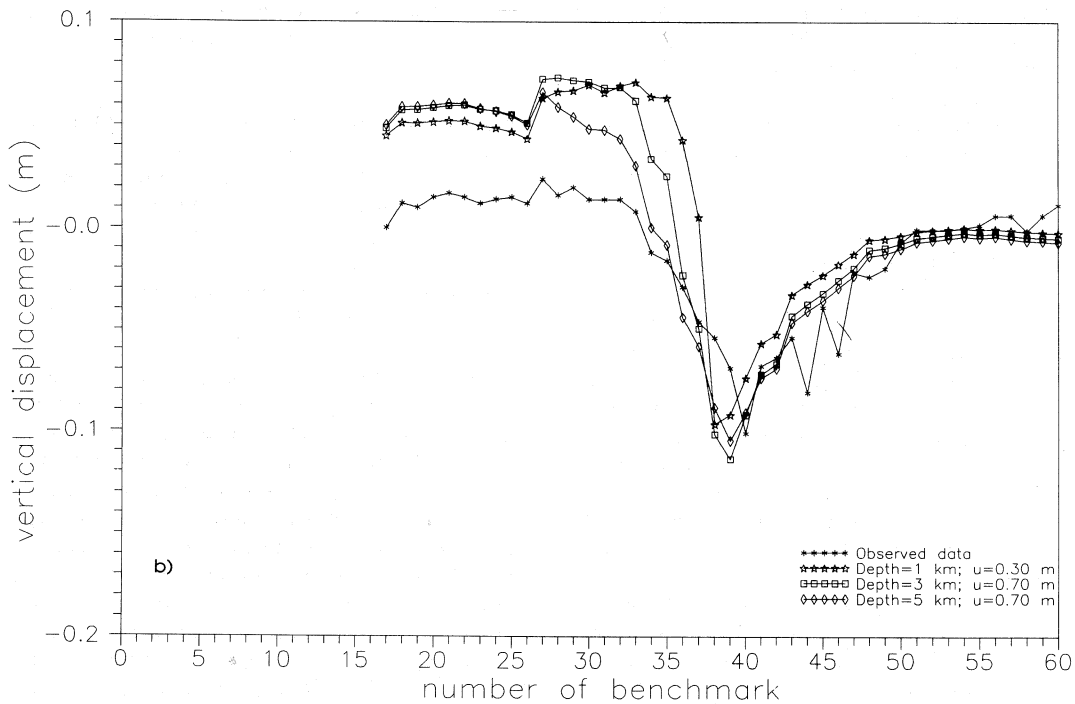
vertical displacement (m)
0.1
−0.0
−0.1
−0.2
0
5
10
15
20
25
30
35
40
45
50
55
60
number of benchmark
b)
Observed data
Depth=1 km; u=0.30 m
Depth=3 km; u=0.70 m
Depth=5 km; u=0.70 m

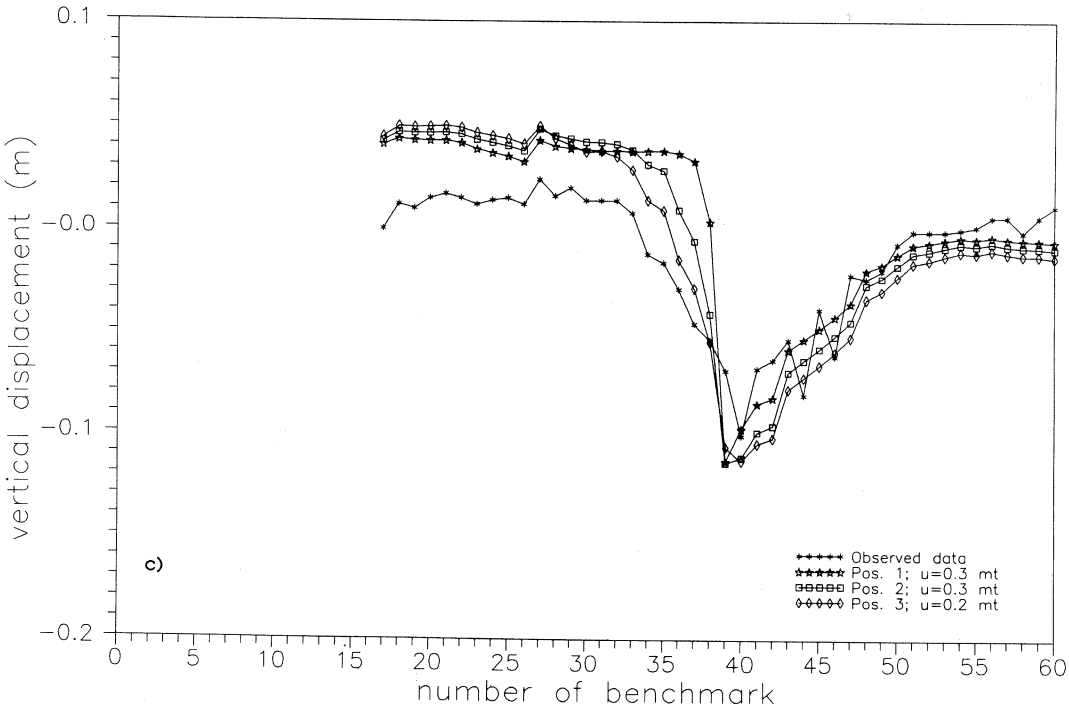

Fig. 4. Effect of the depth on the theoretical displacements (dashed lines) along the Eboli-Potenza line, for a fault dipping 60°, for the three different positions of the southern termination of the fault of fig. 3b). a) Position 1; b) position 2; c) position 3.

the fault width as 10 or 15 km. Many tests have been performed, by sampling the strike-dip parameter space, for various positions of the fault middle point (and various choices for the length and width parameters). The dislocation D has been computed as the best one for each model, in a least squares sense, taking the value

$$D = \frac{\sum_{i=1}^{N} t_i o_i}{\sum_{i=1}^{N} t_i^2}$$

where o_i are the observed data, t_i the theoretical data computed using unit dislocation, and N the number of data.

In fig. 5b) the most significant contour map of the sum of squares residuals are shown, among all the tests performed by varying the central point of the fault. The middle point location chosen for this map (shown in fig. 5a)) is the point of highest gradient of deformation. On the map the zones corresponding to a graben model (1) and to the orthogonal fault (2) are indicated (fig. 5a)). It is evident that the best model is for a strike 110° ± 10°, with the sum of square residuals equal to 0.10 m^2 (for values just out of this range the sum of square residuals is double), which corresponds better to a graben model, whereas values of residuals for models close to the orthogonal fault are several times larger. In principle, such residuals should be compared to the noise actually present in the data set. However, as discussed by De Natale and Pingue (1991), the theoretical measurement errors are generally much lower than the actual errors, mainly due to approximations in the theoretical model (assumption of perfectly planar faults, homogeneous elastic medium, etc.), as reflected in the amount of residuals. So, the minimum residual itself is the best indicator of the noise contained

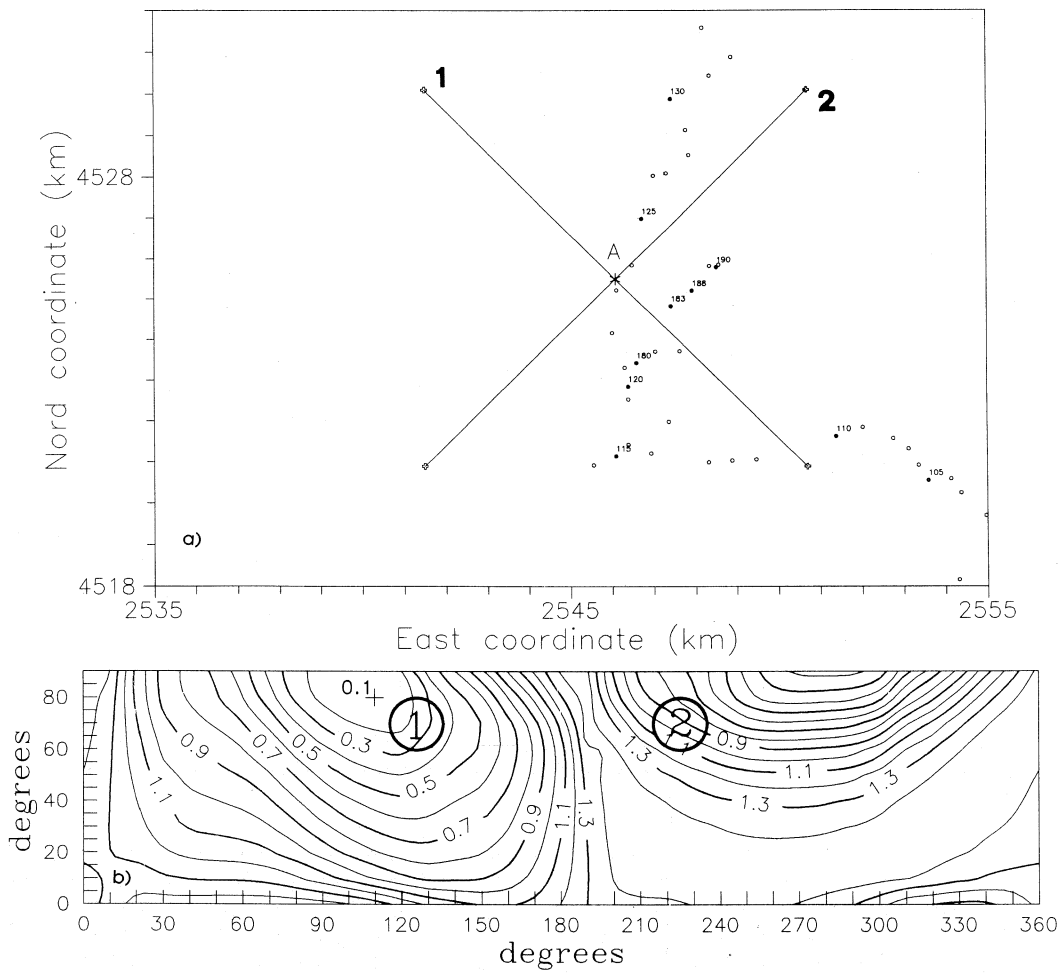

Fig. 5. a) Sketch of the two kinds of fault models proposed for the 40 s subevent. Model 1 corresponds to a fault parallel to the 0 s one (graben model in Bernard and Zollo, 1989). Model 2 corresponds to a fault orthogonal to the 0 s one (Crosson *et al.*, 1986). b) Contour of the sum of square residuals on the benchmarks n. 100 to 140 and 180 to 192, as a function of strike and dip of the fault model for the 40 s event. Circles show strike-dip ranges corresponding to models 1 and 2. Common fault parameters are length=13 km, depth=1 km.

in the data, in this case 0.10 m^2. Then, geodetic data are able to constrain the strike of the 40 s faulting to within about 10°. Dip is also equivalently well constrained to a value of about 80°.

4. Discussion

The analyses so far performed allow us to address and solve some problems still existing in the proposed models for this earthquake. For the main fault segment (0 s subevent) the proposed model is in good agreement with all the constraints coming from seismological and geological data. This subevent has been recognized (Westaway and Jackson, 1987; Bernard and Zollo, 1989) as composed by 3 main rupture phases. Obviously, geodetic data cannot discriminate among different fracture episodes occurring on the same fault, at different times. So,

Length (km)	Strike (deg)	Disloc. (m)	Dip (deg)	Slip angle (deg)	Width (km)	Depth (km)
			0 s			
25	317	1.4	60	-90	20	1
			18 s			
22	310	0.3	20	-90	14	1
			40 s			
13	115	0.7	80	-90	10	1

Table I. Parameters of the fault model.

our model represents the sum of the contributions of all the fracture on the fault plane. It is noteworthy, however, that the total fault length (25 km) is in good agreement with the total duration (about 10 s) of the three fracture episodes (assumed to have occurred on adjacent fault planes) for a rupture velocity of 2.5 km/s (Bernard and Zollo, 1989). The total moment of the 0 s subevent, as computed by levelling data, is 1.9×10^{19} Nm, about 50% higher than the estimate of Westaway and Jackson, based on modeling of WWSN seismological data (1.3×10^{19} Nm). Pantosti and Valensise (1990) also estimated, from geologically observed fault scarps, a similar total moment for the 0 s subevent (1.25×10^{19} Nm). It is important to point out, however, that the long-period centroid-moment tensor computed by several authors gave for the mainshock a global moment of about $(2.5 \div 2.7) \times 10^{19}$ Nm (Boschi *et al.*, 1981; Kanamori and Given, 1982; Westaway and Jackson, 1987). With our estimate of the moment of the first subevent, the total moment of the 23 November earthquake is about 2.6×10^{19} Nm, in agreement with results from centroid-moment tensor inversion of long-period seismic waves. We have, at present, no simple explanation for the disagreement of Westaway and Jackson results based on direct modeling of WWSN data. On the contrary, the estimates by Pantosti and Valensise are likely to be biased from too strong assumptions. In fact, estimating seismic moment from measurements of fault scarps, one implicitly assumes that they exactly match slip at depth. Actually, this very strong assumption can be easily rejected by at least two kinds of arguments. Firstly, their measurements of fault scarps were performed at the end of 1986–beginning of 1987, *i.e.* more than 6 years after the earthquake. So, the inferred values can be biased by man-made alterations (some of them reported by the same authors) and can only represent indicative values of the true ones. Secondly, as largely demonstrated for many worldwide earthquakes, slip on faults producing large earthquakes is far from being homogeneous with depth (Ward and Barrientos, 1986; Harris and Segall, 1987; Ward and Valensise, 1989; De Natale and Pingue, 1991). Moreover, slip at surface is probably the least representative of the average slip, because of the possible anomalous behavior of near-surface layers (in this case, several sedimentary basins are present, like the Ofanto and Sele valleys). Good examples of large discrepancies between surface slip and slip at depth are shown in Harris and Segall, 1987 and Ward and Barrientos, 1986. The latter involved the analysis of a large normal faulting earthquake (Borah Peak, 1983). Pantosti and Valensise also claimed to have checked the coherence of their model with the levelling data. The direct comparison has been performed by us, using their preferred model, and shows a large underestimation (more than 0.2 m) of the maximum subsidence along the Potenza-Grottaminarda lines (fig. 6), which is due to the underestimation of the total moment on the main fault. Concerning the 20 s subevent, we assume herein that the location given by Bernard and Zollo (1989) is correct, and associate it to the zone of S. Gregorio Magno. Once this assumption is accepted, two arguments can be used to constrain its dip to a low-angle one (at least at a certain depth). The first argument is the focal mechanism computed by Westaway and Jackson from teleseismic body waves.Their solution was poorly determined for the rake, but the low-angle dip was well con-

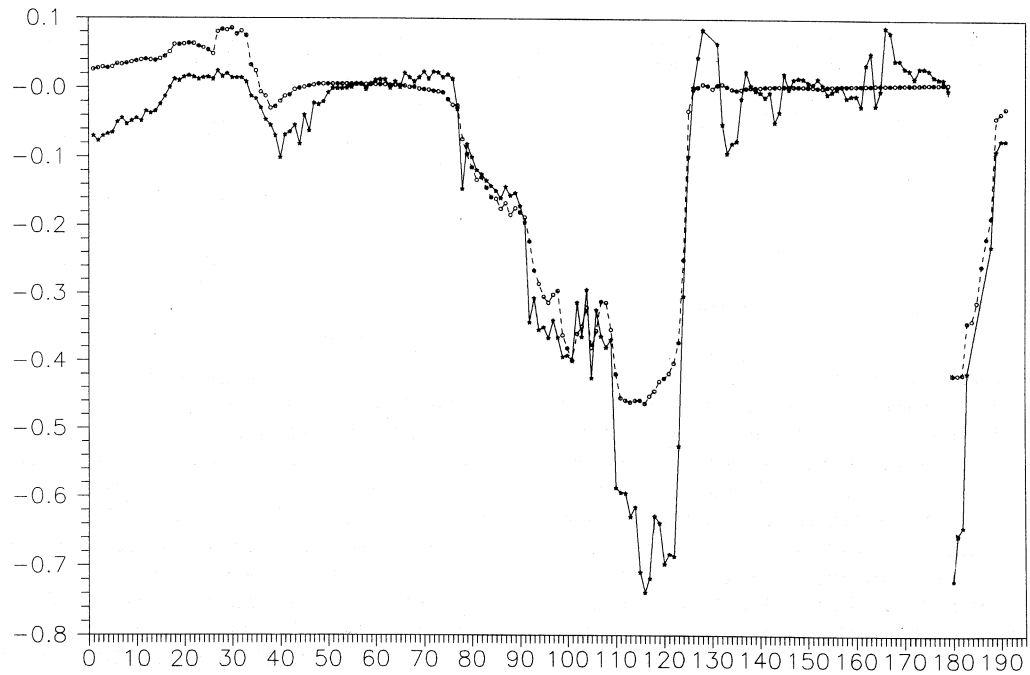

Fig. 6. Fit of theoretical (solid line) to observed (dashed line) data with the fault model proposed by Pantosti and Valensise (1990).

strained by two stations at least (Westaway and Jackson, 1987). The second constraint comes from modeling of vertical ground deformations. As shown, a fault dipping 60° NE and ending north of the Eboli-Potenza levelling line (as assumed by Pantosti and Valensise, 1990) is not consistent with the observed data. Pantosti and Valensise (1990) mantained that a low signal-to-noise ratio is associated with these data. On the contrary, excluding benchmarks from 1 to 16, lying largely on a valley affected by a well-known long-term subsidence, ground displacements located close to the fault zone are very well correlated and very constraining for the southernmost fault structures. As demonstrated in this paper, the only way to hypothesize a 60° dip is to assess that the southern fault termination is located several kilometers south of the Eboli-Potenza line with a depth > 4 km. Such hypothesis was excluded by Pantosti and Valensise (1990), who claimed that south of the line a different seismotectonic domain is present, associated to the 1857 earthquake. The only way to hypothesize for this event a high-angle dip and fault termination north of the levelling line, in agreement with geodetic data, is to assume that in this zone levelling data are biased by a large nontectonic subsidence (about 0.1 m), superimposed to local sliding phenomena (forming the gentle, well-correlated subsidence of bench marks n. 33 to 48). We do not believe such hypothesis is realistic.

Concerning the 40 s subevent, we give in this paper a well-constrained solution for the fault plane, obtained by adding a small levelling data set located close to this fault, and not used in previous studies. The inclusion of this data set eliminates the indeterminacy in fault strike and definitively supports the graben model hypothesis, formulated by Bernard and Zollo (1989) and reported in the model of Pantosti and Valensise (1990), against the orthogonal fault model by Crosson *et al.* (1986). We believe that now a very precise fault model for this complex Apenninic earthquake can be reliably formulated, consistent with all the available data sets. The main ques-

tions that remain still open are the disagreement between the total seismic moment computed from geodetic data (and long-period seismic data) and by teleseismic body wave modeling, and the northern fault termination of the main-shock, given the diffuse aftershock occurrence up to the northernmost levelling line, where on the contrary no significant deformation is observed.

5. Conclusions

Although the 1980 Irpinia earthquake has been very well studied using several data sets, some questions remained not well answered yet. The vertical ground deformation data, analyzed in this paper, had already proven to be a powerful tool to infer the geometrical features of the main fault mechanism. In this paper we have shown that the information content which is actually present in these data also allows us to give strong constraints on more detailed features of the fracture process.

It is important to stress that, used alone, this data set is not well constraining on the faulting location and mechanism, mainly because the levelling lines run almost parallel to the main fault. However, when used in the framework of a multi-disciplinary approach, *i.e.* using joint constraints coming from different data sets, it represents a powerful tool for modeling purposes. Then, one of the aims of future geodetic research in Italy should be to develop the monitoring of active areas, to understand their behavior during inter-seismic (pre- and post-seismic deformations) as well as co-seismic regimes. Such monitoring can in fact shed new light on the seismotectonics of these areas, and can be also used for mid-term earthquake prediction.

REFERENCES

ARCA, S., V. BONASIA, F. PINGUE, R. SCARPA, R. GAULON and J.C. RUEGG (1983): Ground movements and faulting mechanism associated to the November 23, 1980 southern Italy earthquake, *Boll. Geod. Sci. Affini*, **42**, 137-147.

BERNARD, P. and A. ZOLLO (1988): Inversion of *S* polarization from near-source accelerograms. Application to the records of the 1980 Irpinia earthquake, in *Seismic hazard in Mediterranean regions*, edited by J. BONNIN *et al.* (Kluwer Acad. Publis., Dordrecht), pp. 59-69.

BERNARD, P. and A. ZOLLO (1989): The Irpinia (Italy) 1980 earthquake: Detailed analysis of a complex normal faulting, *J. Geophys. Res.*, **94**, 1631-1648.

BOSCHI, E., F. MULARGIA, E. MANTOVANI, M. BONAFEDE, A.M. DZIEWONSKI and J.H. WOODHOUSE (1981): The Irpinia earthquake of November 23, 1980 (abstr.), *EOS Transactions A.G.U.*, **62**, 330.

BRIOLE, P. (1986): Inversion of ground deformation produced by the 1980 Irpinia earthquake, D.E.O. Thesis, Inst. Phys. du Globe, University of Paris.

BRIOLE, P. (1990): Doctorat Thesis, Inst. Phys. du Globe, University of Paris.

COTECCHIA, V. (1986): Ground deformations and slope instability produced by the earthquake of 23 November 1980 in Campania and Basilicata, in *Proceedings of International Symposium on Engineering Geology Problems in Seismic Areas, Bari (Italy), 1986*, Vol. 5.

CROSSON R.S., M. MARTINI, R. SCARPA and S.C. KEY (1986): The Southern Italy earthquake of 23 November 1980: an unusual pattern of faulting, *Bull. Seismol. Soc. Am.*, **76**, 395-407.

CROSSON, R.S., M. MARTINI, R. SCARPA and S.C. KEY (1987): Reply to R. Westaway's comment on «The Southern Italy earthquake of 23 November 1980: An unusual pattern of faulting» by CROSSON, R.S., M. MARTINI, R. SCARPA and S.C. KEY, *Bull. Seismol. Soc. Am.*, **77**, 1075-1077.

DEL PEZZO, E., G. IANNACCONE, M. MARTINI and R. SCARPA (1983): The 23 November 1980 Southern Italy earthquake, *Bull. Seismol. Soc. Am.*, **73**, 187-200.

DE NATALE, G., M. MARTINI and E. TERZINI (1983): Il terremoto del 23 novembre 1980: spostamento su due faglie ortogonali collegate a movimento di blocchi verticali, in *Atti II Convegno G.N.G.T.S.*, pp. 393-406.

DE NATALE, G., R. SCARPA and E. TERZINI (1985): Earthquake location inverse problem: an aftershock analysis of the southern Italy 23 November 1980 earthquake, *Nuovo Cimento C*, **8**, 1-25.

DE NATALE, G., F. PINGUE and R. SCARPA (1988): Seismic and ground deformation monitoring in the seismogenetic region of the southern Apennines, Italy, *Tectonophysics*, **152**, 167-178.

DE NATALE, G. and F. PINGUE (1991): A variable slip fault model for the 1908 Messina Straits (Italy) earthquake by inversion of levelling data, *Geophys. J.*, **104**, 1, 73-84.

FUNICIELLO, R., D. PANTOSTI and G. VALENSISE (1988): Ricostruzione della geometria di faglia del terremoto del 23 novembre 1980 attraverso lo studio della sua espressione superficiale, in *Atti VII Convegno G.N.G.T.S.*, pp. 563-574.

HARRIS, R.A. and P. SEGALL (1987): Detection of a locked zone at depth on the Parkfield, California, segment of the San Andreas fault, *J. Geophys. Res.*, **92**, 7945-7962.

KANAMORI, H. and J.W. GIVEN (1982): Use of long period surface waves for rapid determination of earthquake source parameters. 2 : Preliminary determination of source mechanisms of large earthquakes ($M_S \geq 6.5$) in 1980, *Phys. Earth Plan. Inter.*, **30**, 260-268.

PANTOSTI, D. and G. VALENSISE (1990): Faulting mechanism and complexity of the 23 November 1980, Campania-Lucania earthquake, inferred from surface observations, *J. Geophys. Res.*, **95**, 15319-15341.

WARD, S.N. and S.E. BARRIENTOS (1986): An inversion for slip distribution and fault shape from geodetic observa-

tions of the 1983,Borah Peak, Idaho, earthquake, *J. Geophys. Res.*, **91**, 4909-4919.

WARD, S.N. and G.R. VALENSISE (1989): Fault parameters and slip distribution of the 1915, Avezzano, Italy earthquake derived from geodetic observations, *Bull. Seismol. Soc. Am.*, **79**, 3,690-710.

WESTAWAY, R. (1987): Comment on *The Southern Italy earthquake of 23 November 1980: An unusual pattern of faulting*, by CROSSON, R.S., M. MARTINI, R. SCARPA and S.C. KEY, *Bull. Seismol. Soc. Am.*, **77**, 1071- 1074.

WESTAWAY, R. and J. JACKSON (1984): Surface faulting in the Southern Italian Campania-Basilicata earthquake of 23 November 1980, *Nature*,**312**, 436-438.

WESTAWAY, R. and J. JACKSON (1987): The earthquake of 1980 November 23 in Campania-Basilicata (Southern Italy), *Geophys. J.R. Astron. Soc.*, **90**, 375-443.